

EVALUATION OF GROUND FAILURE PROBABILITY CAUSED BY SOIL LIQUEFACTION FOR BOGURA SADAR, BANGLADESH

Md. Mahabub Rahman^{*1}, Md. Belal Hossain², Md. Aminul Islam³ and Md. Sohanoor Rahaman⁴

¹ Lecturer, Department of Civil Engineering, Hajee Mohammad Danesh Science and Technology University, Bangladesh, e-mail: mmr.civil@hstu.ac.bd

² Associate Professor, Department of Civil Engineering, Hajee Mohammad Danesh Science and Technology University, Bangladesh, e-mail: mbh.civil@hstu.ac.bd

³ Assistant Professor, BUET-Japan Institute of Disaster Prevention and Urban Safety, Bangladesh University of Engineering and Technology (BUET), Bangladesh, e-mail: aminul0804043@gmail.com

⁴ Lecturer, Department of Civil Engineering, City University, Bangladesh, e-mail: mdsohanoorrahaman2000@gmail.com

***Corresponding Author**

ABSTRACT

Nowadays, the term "earthquake" refers to a catastrophic occurrence that causes destruction worldwide. Bogura Sadar Upazila is vulnerable to soil liquefaction during seismic activity because of its location. This research aims to determine the probability that liquefaction may result in ground failure in Bangladesh's Bogura Sadar upazila. The article employs a simplified methodology predicated on the blow count of the standard penetration test (SPT) to evaluate the potential for liquefaction-induced ground failure. To reach the research goal, 153 borehole data points were used to figure out how likely the study region was to liquefy in an earthquake with a magnitude of 6.5. The findings are presented as hazard maps that depict the probabilities of ground failure (PG), the liquefaction potential index (LPI), and safety factors (FS). The results show that 0.94% of the research area is very high risk for ground collapse because of liquefaction if there is a 6.5 magnitude earthquake. The LPI result shows that 1% of places are very likely to liquefy, and 34% are likely to do so. In addition, 7.65% and 30.22% of the study area's regions were classified as being at high and moderate risk of ground collapse in the previously mentioned earthquake scenario, respectively. The 6 m depth is the most dangerous for the factor of safety, with 23.96% of the research area's FOS falling below 1.0. This means that there is a much higher risk of liquefaction. The hazard maps made for Bogura Sadar are critical for reaching long-term development goals.

Keywords: *Earthquake, Liquefaction, Ground Failure Probability, SPT-N, Bogura Sadar*

1. INTRODUCTION

Bangladesh frequently experiences natural disasters due to its geographical location and the geological characteristics of the region. Due to their proximity to the Indian and Eurasian plates' convergent plate boundary, Bangladesh and its surrounding regions are prone to earthquakes (Hossain et al., 2022; Rahman et al., 2025). Liquefaction is one of the worst things that can happen during an earthquake because it can hurt people and buildings very badly (Rahman et al., 2020). The main danger is earthquakes, and liquefaction is a secondary danger that can happen when the ground shakes. This process makes soil sediments below the water table weaker for a short time and makes them act more like thick liquids (Lee et al., 2004). Researchers from all over the world have done a lot of work on mapping liquefaction vulnerabilities. In developing countries, liquefaction and mitigation have become critical concerns. A number of researchers investigated the causes of liquefaction and suggested correlations to assess liquefaction, taking into account a variety of parameters (Rahman et al., 2023).

Some researchers used probabilistic and deterministic methods, while others stressed how important deep learning and machine learning are for figuring out how soil liquefaction works. Abdullah & Aal's (2021) study aimed to assess and delineate the vulnerability of Jeddah City to liquefaction. The LPI was calculated using data from 214 SPT boreholes. The findings indicate that the majority of Jeddah is situated in a region with a comparatively low liquefaction potential [6]. The districts of Abhur and Al-Hamra are the only locations where it is moderate to high. A similar case study was conducted by Wadi et al. (2021) at a sugar plant location in the Upper Benue area of Nigeria to evaluate subsoil deposition for soil liquefaction assessment. The latest case study conducted by Subedi and Acharya (2022) aimed to assess the liquefaction potential in the Kathmandu Valley, Nepal. This evaluation utilized borehole data that incorporated SPT-N values from 410 different locations. Several studies have investigated the susceptibility to soil liquefaction in different cities across Bangladesh. Fahim et al. (2022) looked at how likely it was for Dhaka, the capital of Bangladesh, to liquefy, and Rahman et al. (2025) looked at how likely it was for Dinajpur, a city in the northwest, to do the same. Hasan et al. (2025) looked at Chittagong's vulnerability, and Ansary et al. (2022) looked at Sylhet's vulnerability. Hossain and Rahman (2025) looked at how likely Bogura was to liquefy, and Ashikuzzaman et al. (2023) looked at how likely Rajshahi was to liquefy. Many researchers have utilized machine learning algorithms to evaluate soil liquefaction susceptibility. Sayed & Rahman (2025) utilized the M5 algorithm, while Rahman et al., (2025) implemented four SVM kernel functions. Hanandeh et al., (2022) applied support vector machines, Quadratic Discriminant Analysis, and Decision Trees. Kumar et al., (2024) employed Relevance Vector Machine and Genetic Programming to assess the catastrophic event.

This study is the first assessment of ground failure probability (PG) in Bogura Sadar due to soil liquefaction. As the study area's soil is sandy with high GWT and positioned in a seismically active zone, this area is particularly vulnerable to liquefaction. Reliable urban development requires an evaluation of the city's liquefaction hazards. Using the FS and LPI, we evaluate the liquefaction potential for different layers below the earth's surface of the study region. The FS is determined using Idriss & Boulanger (2008), while the LPI is calculated using Iwasaki et al. (1982). This study uses an estimated site-specific PGA value and an earthquake magnitude of 6.5. Then, using an empirical approach presented by Li et al. (2006), PG is determined from LPI. Ultimately, all numerical information is used to generate interpolated maps utilizing GIS software.

2. STUDY AREA

Bogura sadar is situated in the northern region of Bangladesh, inside the district Bogura, as seen in Figure 1. The coordinates are 24°51' N and 89°22' E.

2.1 Data Collection

Soil investigation reports from 153 sites were gathered from various organizations, both private and public, to meet the goals of the study. Various soil index properties test results, including the SPT-N

value, which is essential for assessing liquefaction risk, are included in soil investigation reports. The locations of the data points that encompass the Bogura Sadar are depicted in Figure 1.

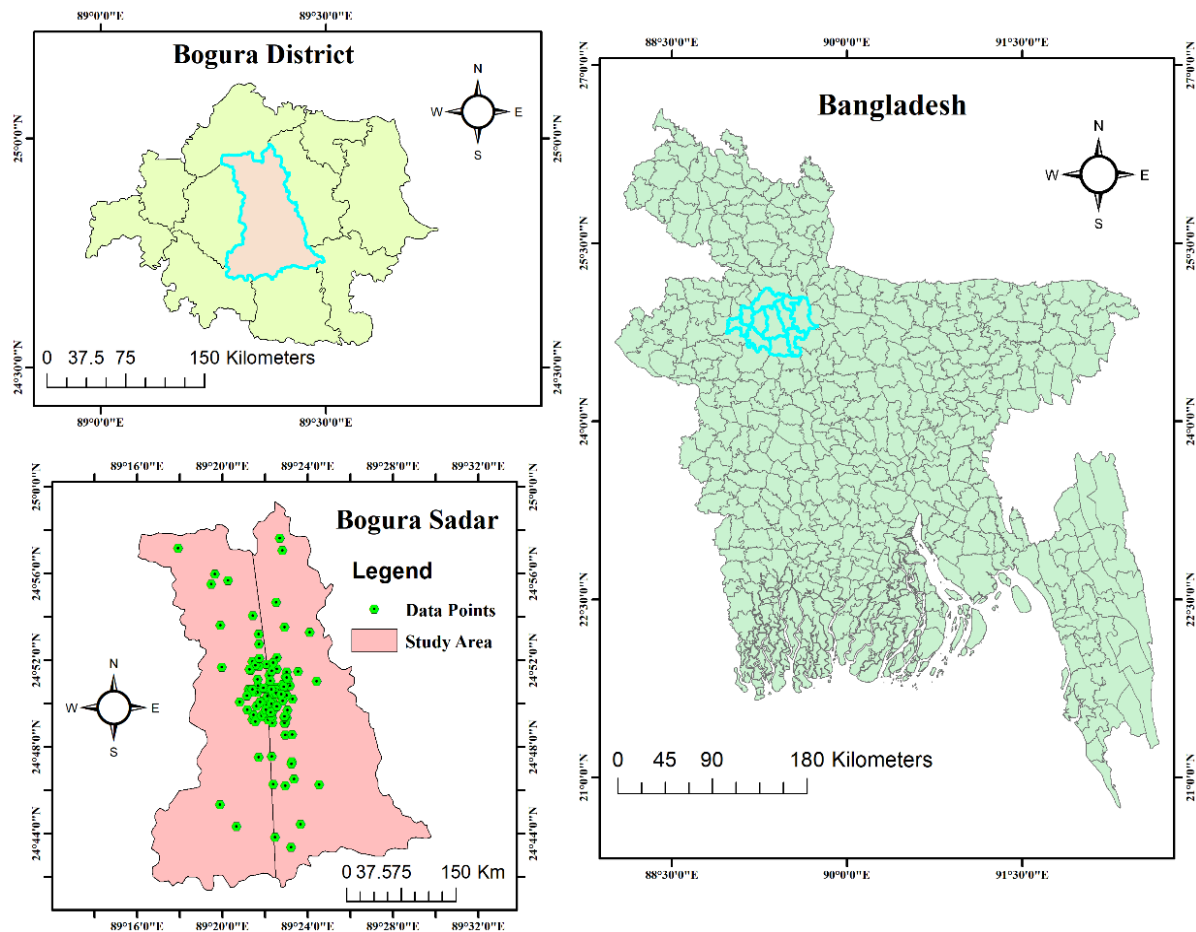


Figure 1: Study area map with data points

2.2 Geomorphological and Hydrological Condition

An essential component in soil liquefaction is groundwater. During an earthquake, liquefaction is more probable because of the shallow groundwater level, which lowers the effective confining stress at any depth (Jalil et al., 2021). Figure 2a displays the groundwater level of the research region on a geographic map. The research area's soil is very vulnerable to liquefaction during seismic events since groundwater is located there at shallow depths between 0.10 and 6.1 meters below the ground surface. The Bogura District's surface geology map is shown in Figure 2b. According to the map, the Bogura area is mostly covered with four different kinds of soil. Alluvial sand, alluvial silt, alluvial silt and clay, and clay residuum are the different forms of soil. Fine silt and clay particles combine to form alluvial silt and clay soils (Rahman, 2025). With a comparatively larger percentage of clay particles, they have characteristics of both silt and clay soils. This kind of soil covers 23.1% of the Bogura district's total area. Another kind of soil that covers 26.9% of the Bogura district is alluvial silt. It is made up of tiny particles that are bigger than clay but smaller than sand. With little to no movement or deposition, clay residuum was created by the weathering and breakdown of parent rock material. In the Bogura district, this kind of soil covers 49.4% of the surface area.

2.3 Seismicity

Five major faults are crucial for the occurrence of devastating earthquakes in terms of geology and plate tectonics. One kind of gravity fault is the Bogra fault. It is quite close to the Jamuna River and the town of Bogra. Most people agree that Bogura is seismically stable. Major tectonic plate borders, which are

usually linked to strong seismic activity, are not close to the district. Because of this, Bogura has comparatively mild seismicity in comparison to other earthquake-prone areas. But it's crucial to remember that Bangladesh is located in the Bengal Basin, an area that is prone to earthquakes. Significant seismic activity has historically occurred in the Bengal Basin, which is situated where the Indian and Eurasian tectonic plates collide. Bogura Sadar is located in a moderately seismically dangerous area, not a high-risk one. Bogura Sadar is located in zone 3 with a zone coefficient of 0.28 on the seismic zonation map (BNBC, 2020).

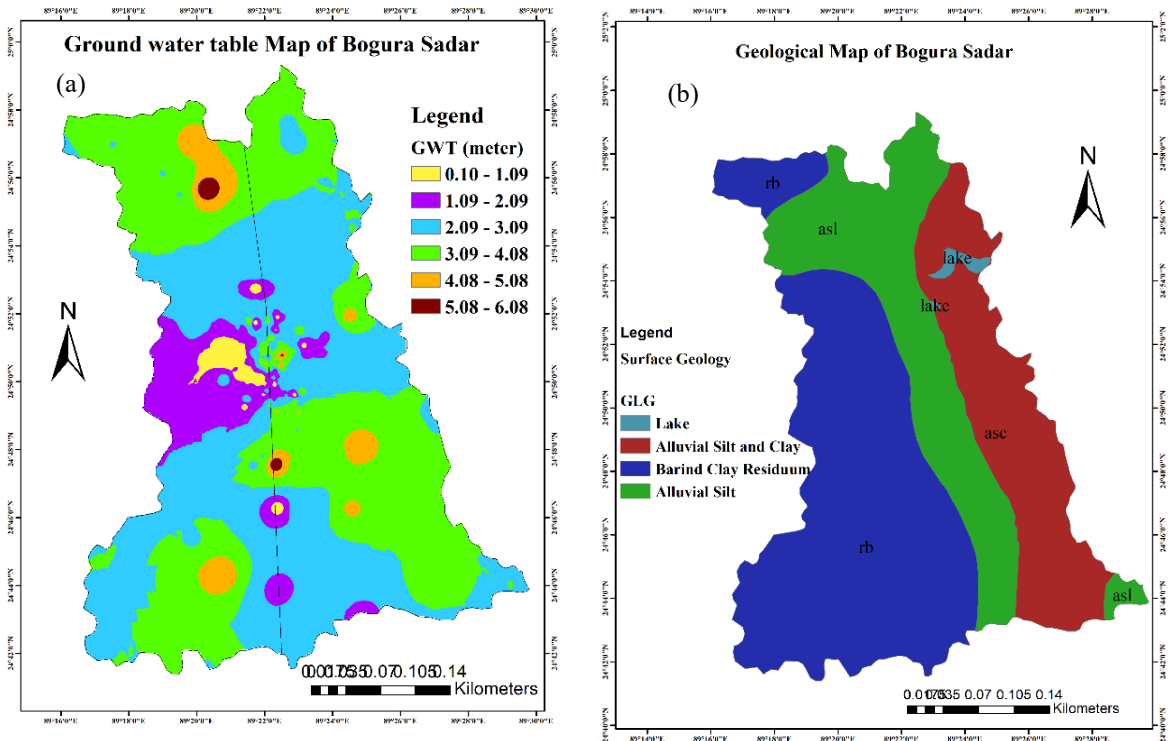


Figure 2: Map of Bogura district (a) ground water table and (b) surface geology

3. METHODOLOGY

3.1 Evaluation of Ground Failure Probability

Equation 1 as given by Li et al., (2006) was utilized to determine the ground failure probability (PG) due to liquefaction in order to perform a quantitative evaluation.

$$P_G = \frac{1}{1 + e^{4.71 - 0.71 * LPI}} \quad (1)$$

where LPI represents the liquefaction potential.

3.2 Estimation of the LPI

Equation 2 from Iwasaki et al. (1982) is used to calculate the LPI for the research area up to a depth of 12 meters below the earth.

$$LPI = \int_0^z F(z)W(z)dz \quad (2)$$

where z = layer thickness; $F(z)$ = function of FOS and obtained by:

when $FS \leq 1$ then $F(z) = 1$

when $FS > 1$ then $F(z) = 0$

In the above equation,

$$W(z) = 10 - 0.5z$$

Table 1 illustrates how the susceptibility to liquefaction may be divided into several groups based on the LPI and PG value.

Table 1: Risk level categorization based on PG by Li et al., (2006) and LPI by Iwasaki et al., (1982)

Level of risk	In terms of PG	In terms of LPI
Little or no risk	PG < 0.1	0
Low risk	0.1 < PG < 0.3	0-5.0
Medium risk	0.3 < PG < 0.7	-
High risk	0.7 < PG < 0.9	5.0-15.0
Extremely high risk	PG > 0.9	>15

3.3 Determination of the FOS

This study determines FS using Equation 3 as provided by Idriss & Boulanger (2008).

$$FS = \frac{CRR_{7.5}}{CSR} * MSF * K_{\sigma} \quad (3)$$

Here, $CRR_{7.5}$ denotes the cyclic resistance ratio at $M_w = 7.5$. The MSF and K_{σ} were computed by the Equations 4-5.

$$MSF = 6.90e^{\frac{-M_w}{4}} - 0.058 (\leq 1.8) \quad (4)$$

$$K_{\sigma} = 1 - C_{\sigma} \ln\left(\frac{\sigma_v'}{P_a}\right) (\leq 1.1) \quad (5)$$

The C_{σ} can be calculated utilizing Equation 6.

$$C_{\sigma} = \frac{1}{18.9 - 2.55\sqrt{(N_1)_{60}}} (\leq 0.3) \quad (6)$$

The CRR was computed using the N value adjusted for field procedures and overburden pressure, whereas the unadjusted SPT-N value was modified according to Equation 7 (BNBC, 2020).

$$(N_1)_{60} = N C_N C_E C_B C_R C_S \quad (7)$$

In equation 7, $(N_1)_{60}$ is modified field N value.

The $CRR_{7.5}$ is assessed using Equation 8.

$$CRR_{7.5} = \exp\left(\frac{(N_1)_{60cs}}{14.1} + \left(\frac{(N_1)_{60cs}}{126}\right)^2 + \left(\frac{(N_1)_{60cs}}{23.6}\right)^3 + \left(\frac{(N_1)_{60cs}}{25.4}\right)^4 - 2.8\right) \quad (8)$$

Here, $(N_1)_{60cs}$ is the corrected field N.

Equations 9 and 10 are followed to determine $(N_1)_{60cs}$:

$$(N_1)_{60cs} = (N_1)_{60} + \Delta(N_1)_{60} \quad (9)$$

$$\Delta(N_1)_{60} = \exp\left(1.63 + \frac{9.7}{FC+0.01} - \left(\frac{15.7}{FC+0.01}\right)^2\right) \quad (10)$$

In the aforementioned equation, FC denotes the finer percentage. The CSR is then calculated using Equation 11 (Idriss & Boulanger, 2008; BNBC, 2020).

$$CSR = 0.65 \frac{\tau_{max}}{\sigma_v'} = 0.65 \frac{a_{max}}{g} \frac{\sigma_v}{\sigma_v'} r_d \quad (11)$$

Where, ' a_{max} ' is the PGA, σ_v and σ_v' are the overburden stresses. The factor r_d can be calculated utilizing the Equation 12.

For, $z \leq 34m$,

$$r_d = \exp[\alpha(z) + \beta(z)M] \quad (12)$$

In the above equation,

$$\alpha(z) = -1.012 - 1.126 \sin[(z / 11.73) + 5.133]$$

$$\beta(z) = 0.106 + 0.118 \sin[(z / 11.28) + 5.142]$$

Where ‘z’ is the soil layer thickness (m). Sonmez (2003) indicated that soils may be liquefied within the range of FS 1 to 1.2. The risk level in the Bogura District has been categorized according to the FS values as follows:

- ✓ FS > 1.2: Safe
- ✓ 1.0–1.2: Moderate risk
- ✓ FS < 1.0: High risk

4. RESULTS AND DISCUSSION

4.1 Factor of Safety Variation

The factor of safety determination at different subsoil layers (0-12 m) for data point-34 as a sample is shown in Table 2, using the procedures outlined in the methodology section. Figure 3a-d presents interpolation maps illustrating the spatial spread of FS values throughout the study area at depths of three, six, nine, and twelve meters. The FS and LPI maps of the research area were generated using ArcGIS software. All maps used the conventional IDW interpolation method. These liquefaction hazard maps illustrate the potential for liquefaction across different soil strata. Figure 3 illustrates that the average FS values in the research region attain their minima (below 1.2) for the majority of drilling sites at depths of three and six meters, indicating a considerable vulnerability to liquefaction. The red hues of the legends in Figures 3a–d represent the lowest FS (below 1.0).

Table 2: FS determination using Mw = 6.5 for data point-34

Soil Strata	(N ₁) ₆₀	(N ₁) _{60CS}	C _N	σ _v (kN/m ²)	σ' _v (kN/m ²)	r _d	CSR	CRR _{7.5}	MSF	CRR	FOS
0-1.5	3	13.38	2.61	24.45	14.64	0.99	0.30	0.14	1.14	0.16	0.54
1.5-3	9	23.43	1.99	49.8	25.275	0.97	0.35	0.26	1.14	0.29	0.85
3-4.5	11	23.81	1.66	75.45	36.21	0.94	0.36	0.26	1.14	0.30	0.85
4.5-6	10	19.95	1.46	100.95	46.995	0.91	0.36	0.21	1.14	0.23	0.66
6-7.5	20	31.34	1.30	127.95	59.28	0.88	0.35	0.58	1.14	0.67	1.92
7.5-9	27	37.05	1.17	156	72.615	0.85	0.33	1.77	1.14	2.02	6.08
9-10.5	30	36.75	1.08	184.5	86.4	0.82	0.32	1.65	1.14	1.88	5.91
10.5-12	31	35.43	1.00	213.15	100.335	0.79	0.30	1.21	1.14	1.39	4.56

As seen in Figure 3a, the deterministic method was used to compute the FS values for Mw = 6.5 at a depth of 3 meters from the surface of the earth using soil test data collected from many locations within the study area. About 40.39 percent of the research region's FS is less than 1.2 for Mw = 6.5, suggesting liquefaction hazards. The fact that 59.61% of the area has an FS higher than 1.2 indicates that liquefaction is unlikely in such regions. At 6 meters below the surface, Figure 3b displays the FS values for Mw = 6.5. Approximately 23.96% of the area has an FS less than 1.0, suggesting an extremely high risk of liquefaction. However, 59.54% of the research region's FS is higher than 1.2, illustrating that liquefaction is unlikely in such places.

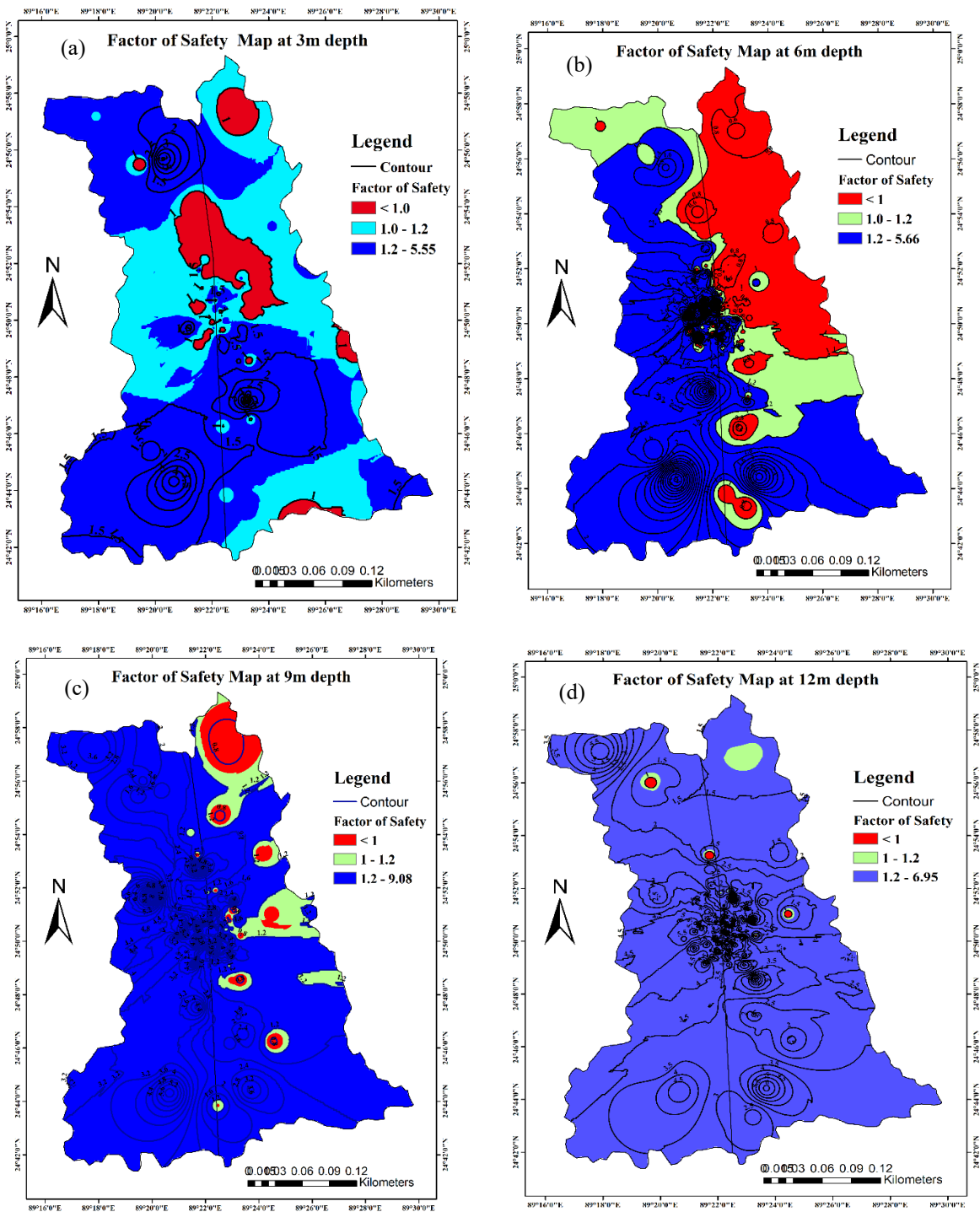


Figure 3: FS contour maps (a) 3m, (b) 6m, (c) 9m and (d) 12 m

FS zonation contour maps for $M_w = 6.5$ are shown in Figures (c–d) at depths of 9 and 12 meters below the surface, respectively. Of the research zone, 88.44% and 98.61% are deemed safe. According to the study's risk maps, the soil layers become less liquefiable as the depth of the soil rises from 9 m to 12 m. A comparative bar diagram illustrating FS at different depths is shown in Figure 4. The graphic unequivocally shows that the portion of the study zone above 59.5% is secure from liquefaction at $M_w = 6.5$ at any depth.

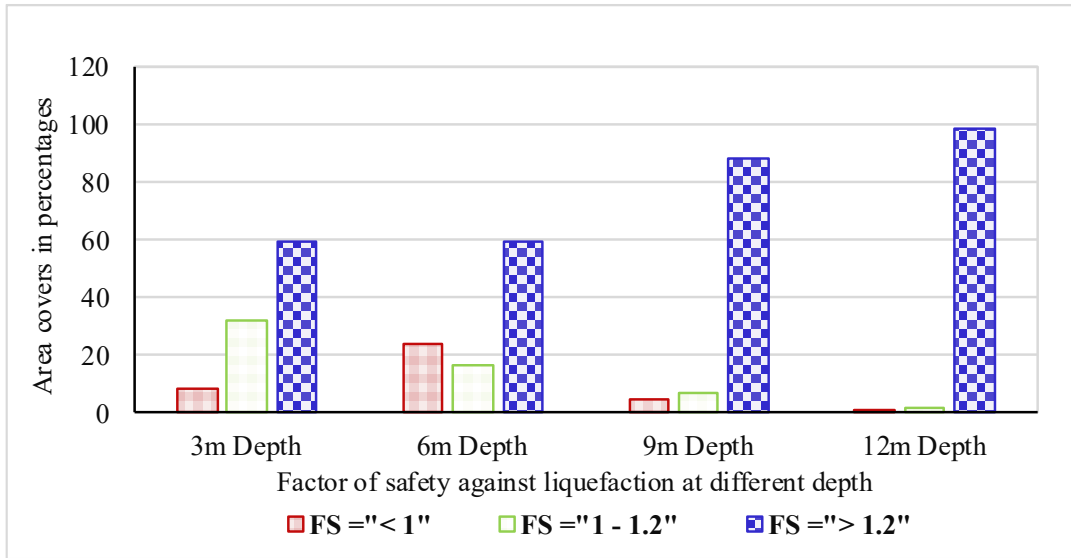


Figure 4: Comparison of FS at different depth

4.2 LPI Contour

Table 3 provides an example of how to calculate LPI, and the LPI values for each of the 153 boreholes were used to construct the LPI zonation contour map of the research region. The IDW interpolated map of the LPI's spatial distribution is shown in Figure 5a, and Figure 5b shows the proportion of the region covered by each liquefaction risk category.

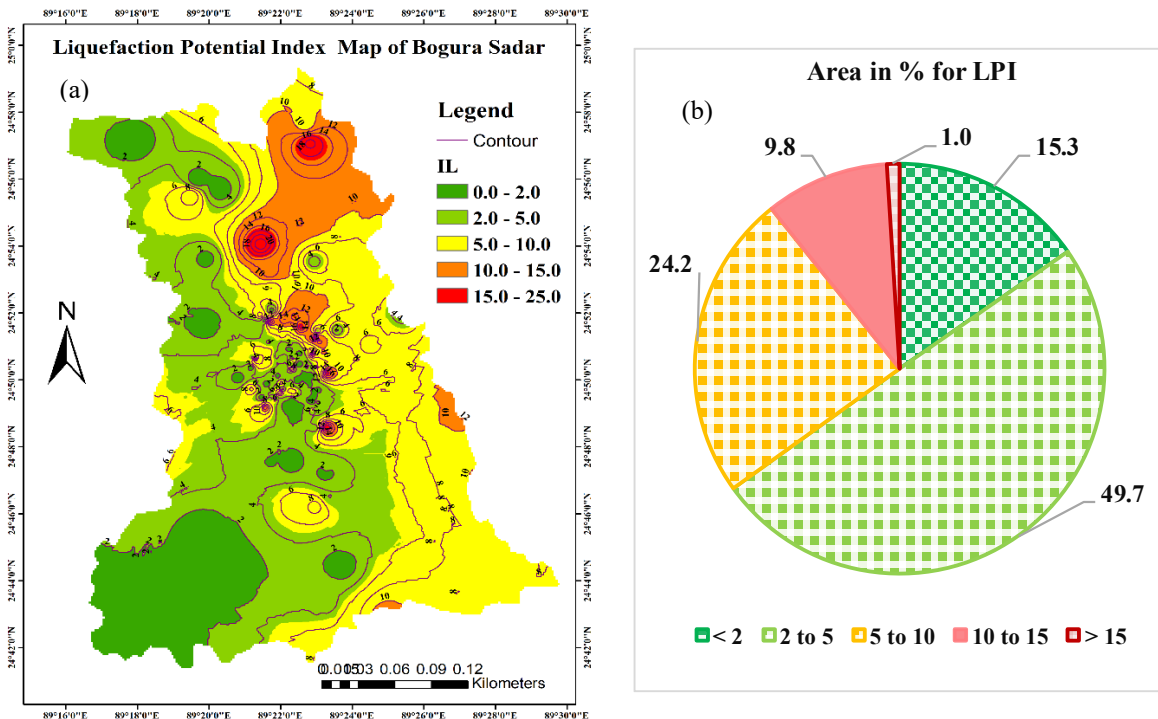


Figure 5: LPI vulnerability map (a) spatial distribution (b) area in percentage

The comparative research indicates that 1% of the sample region is situated in an area with a significantly elevated risk of liquefaction resulting from earthquakes with a magnitude of $M_w = 6.5$. At

6.5 Mw, 34% of the sampled area is categorized as a high liquefaction danger zone, whilst 66% is designated as having a moderate liquefaction hazard.

Table 3: PG determination using Li et al., (2006) for datapoint-34

Soil Strata (m)	FS	F(z)	Thickness of strata, H	W(z)	W(z)*H* F(z)	LPI	PG
1.5	0.54	0.46	1.5	9.625	6.59	14.278	0.99
3	0.85	0.15	1.5	8.875	2.03		
4.5	0.85	0.15	1.5	8.125	1.87		
6	0.66	0.34	1.5	7.375	3.79		
7.5	1.92	0.00	1.5	6.625	0.00		
9	6.08	0.00	1.5	5.875	0.00		
10.5	5.91	0.00	1.5	5.125	0.00		
12	4.56	0.00	1.5	4.375	0.00		

4.3 Probability of ground failure contour

Figures 6(a–b) show the probability map that indicates the risk of ground collapse in the Bogura area due to soil liquefaction for a moment magnitude of 6.5, using IDW interpolation. Table 3 tabulates the computation process for each site. A zone of high danger is shown by the red-highlighted region, while a zone of low risk is indicated by the green area. According to analysis, compared to the other part of Bogura, the northeastern portions show a greater sensitivity to ground collapse. The Bogura district's southwest section exhibits a safe area against ground collapse in the event of an Mw = 6.5 earthquake.

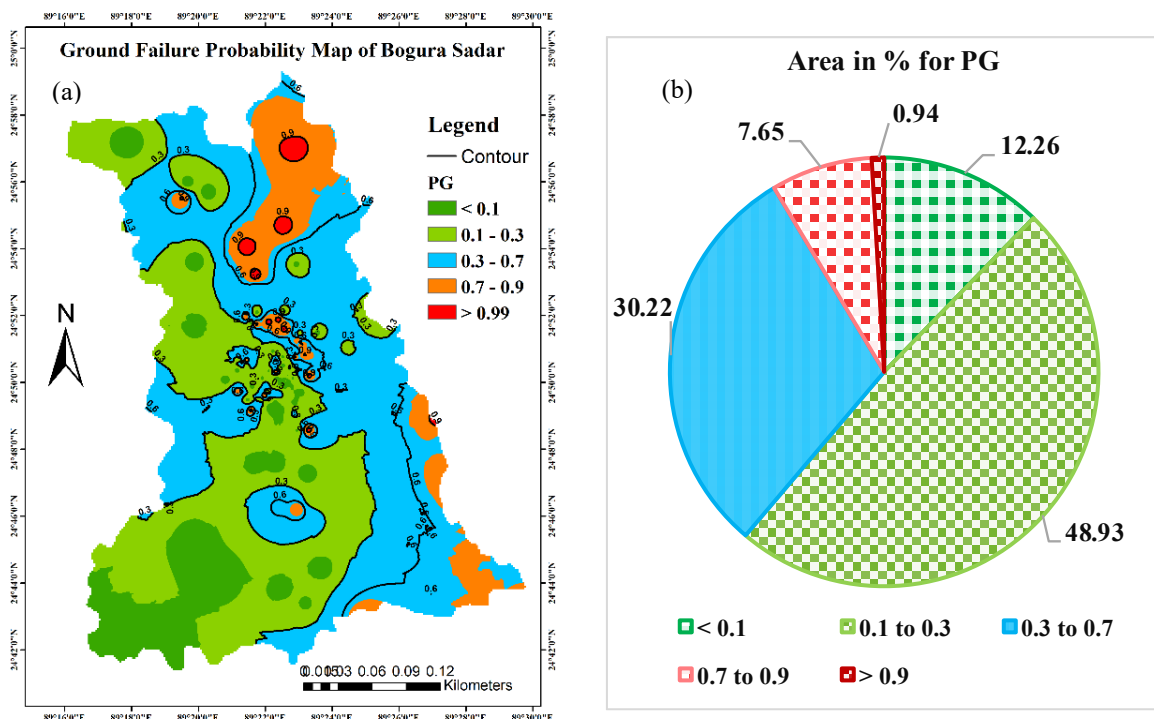


Figure 6: PG vulnerability map (a) spatial distribution (b) area in percentage

In the study area, 0.94% of the entire region is categorized as a very high hazard of ground collapse due to liquefaction following an Mw = 6.5. Furthermore, 7.65% and 30.22% of the research area's expanse are classified as high and moderate risk, respectively (Figure 6b). Conversely, 48.93% of the region is classified as low risk. These findings correspond with the earlier conclusions derived from the examination of FS and LPI.

5. CONCLUSIONS

This study is the first to evaluate the risk that the Bogura District's liquefaction danger may cause a ground collapse. Using the FS and LPI, the research area's sensitivity to subsurface layer liquefaction hazard was evaluated in order to determine the chance of ground collapse. GIS was used to create interpolated contour maps of the computed FS and LPI. Green denotes areas that are safe from liquefaction, whereas red denotes very dangerous areas, according to their color categorization. Here is a summary of the key findings:

- ❖ At a depth of 3 meters, about 40.39 percent of the area's FS is less than 1.2, illustrating liquefaction threats. At 6 meters below the surface, 23.96% of the study area's FOS is less than 1.0, which means there is a very high risk of liquefaction. Nonetheless, 59.54% of the FOS in the study area exceeds 1.2, suggesting that liquefaction is improbable there. Additionally, at depths of 9 and 12 meters below the surface, respectively, 88.44% and 98.61% are considered safe.
- ❖ The spatial interpolation maps created for the research show that the susceptibility of soil liquefaction decreases as the depth rises. This might be explained by the increasing overburden pressure that causes soil stiffness in the soil layers above and below.
- ❖ 34% of the area is in a high liquefaction risk, while 65% is in a low liquefaction hazard region. Based on the LPI value, 1% of the area has an extremely high risk of liquefaction at 6.5 Mw.
- ❖ 0.94% of the investigated area is identified as very high risk of ground collapse due to liquefaction, according to the results of a probability study of ground failure. Additionally, 30.22% and 7.65% of the study area's total area are categorized as moderately and very risky, respectively. On the other hand, 48.93% of the area is categorized as low risk.
- ❖ The government of Bangladesh may consider the interpolated contour maps to be a useful tool for disaster mitigation.

ACKNOWLEDGEMENTS

The authors like to convey their appreciation to the LGED, PWD, EED of Bogura, and several commercial entities for supplying the SPT-N database.

DECLARATION OF USE OF AI

The authors confirmed that no AI tools or technology were used in the preparation of this paper.

REFERENCES

- Hossain, M. B., Roknuzzaman, M., & Rahman, M. M. (2022). Liquefaction potential evaluation by deterministic and probabilistic approaches. *Civil Engineering Journal*, 8(7), 1459-1481. <http://dx.doi.org/10.28991/CEJ-2022-08-07-010>
- Rahman, M. M., Thakur, S., Ahmed, S., & Yasmin, R. (2025). GIS-based development of liquefaction hazard and soil distribution maps for Dinajpur Sadar, Bangladesh. *International Journal of Engineering and Geosciences*, 11(2), 263-273. <https://doi.org/10.26833/ijeg.1662672>
- Rahman, M. A., Ahmed, S., & Imam, M. O. (2020). Rational way of estimating liquefaction severity: an implication for Chattogram, the Port City of Bangladesh. *Geotechnical and Geological Engineering*, 38(2), 2359-2375. <https://doi.org/10.1007/s10706-019-01134-2>
- Lee, D. H., Ku, C. S., & Yuan, H. (2004). A study of the liquefaction risk potential at Yuanlin, Taiwan. *Engineering Geology*, 71(1-2), 97-117. [https://doi.org/10.1016/S0013-7952\(03\)00128-5](https://doi.org/10.1016/S0013-7952(03)00128-5).

- Rahman, M. M., Hossain, M. B., & Roknuzzaman, M. (2023, April). Effect of peak ground acceleration (PGA) on liquefaction behavior of subsoil: A case study of Dinajpur Sadar Upazila, Bangladesh. In AIP Conference Proceedings (Vol. 2713, No. 1). AIP Publishing. doi: <https://doi.org/10.1063/5.0129770>
- Abdullah, G. M., & Abd El Aal, A. (2021). Liquefaction hazards mapping along Red Sea coast, Jeddah city, Kingdom of Saudi Arabia. *Soil Dynamics and Earthquake Engineering*, 144, 106682. <https://doi.org/10.1016/j.soildyn.2021.106682>.
- Wadi, D., Wu, W., Malik, I., Ahmed, H. A., & Makki, A. (2021). Assessment of liquefaction potential of soil based on standard penetration test for the upper Benue region in Nigeria. *Environmental Earth Sciences*, 80(7), 254. <https://doi.org/10.1007/s12665-021-09565-y>.
- Subedi, M., & Acharya, I. P. (2022). Liquefaction hazard assessment and ground failure probability analysis in the Kathmandu Valley of Nepal. *Geoenvironmental Disasters*, 9(1), 1. <https://doi.org/10.1186/s40677-021-00203-0>.
- Fahim, A. K. F., Rahman, M. Z., Hossain, M. S., & Kamal, A. M. (2022). Liquefaction resistance evaluation of soils using artificial neural network for Dhaka City, Bangladesh. *Natural Hazards*, 113(2), 933-963.
- Hasan, M. M., Rahman, M. Z., & Fahim, A. K. F. (2025). Earthquake induced liquefaction hazard analysis for Chittagong City using machine learning. *Geomatics, Natural Hazards and Risk*, 16(1), 2451126.
- Ansary, M. A., Jahan, N., & Ritu, S. (2022). Estimation of liquefaction susceptibility of a new international airport site in Sylhet, Bangladesh. *Pure and Applied Geophysics*, 179(9), 3441-3462.
- Hossain, M. B., & Rahman, M. M. (2025). Seismic Microzonation and Probability of Ground Failure Assessment Caused by Liquefaction for Bogura District, Bangladesh. *Journal of Rehabilitation in Civil Engineering*, 13(2), 218-242. doi: 10.22075/jrce.2024.34111.2086
- Ashikuzzaman, M., Hossain, A., & Salan, M. S. A. (2023). Liquefaction assessment of Rajshahi city corporation, Bangladesh. *Indian Geotechnical Journal*, 53(2), 455-464.
- Sayed, A., & Rahman, M. M. (2025). M5 soft computing techniques for assessment of soil liquefaction. *Journal of Rehabilitation in Civil Engineering*, 13(3), 199-214. doi: 10.22075/jrce.2025.34669.2134
- Rahman, M. M., Hossain, M. B. & Sayed, A. (2025). Prediction of Soil Liquefaction Using Machine learning Approaches. *Engineering Transactions*, 73(2):1-22. <https://doi.org/10.24423/enstrans.3360.2025>
- Hanandeh, S. M., Al-Bodour, W. A., & Hajjij, M. M. (2022). A comparative study of soil liquefaction assessment using machine learning models. *Geotechnical and Geological Engineering*, 40(9), 4721-4734.
- Kumar, D. R., Samui, P., Burman, A., & Kumar, S. (2024). Seismically induced liquefaction potential assessment by different artificial intelligence procedures. *Transportation Infrastructure Geotechnology*, 11(3), 1272-1293.
- Idriss, I. M., & Boulanger, R. W. (2008). *Soil liquefaction during earthquakes*. Earthquake Engineering Research Institute.
- Iwasaki, T., Tokida, K. I., Tatsuoka, F., Watanabe, S., Yasuda, S., & Sato, H. (1982, June). Microzonation for soil liquefaction potential using simplified methods. In *Proceedings of the 3rd international conference on microzonation*, Seattle (Vol. 3, No. 2, pp. 1310-1330).
- Li, D. K., Juang, C. H., & Andrus, R. D. (2006). Liquefaction potential index: a critical assessment using probability concept. *Journal of GeoEngineering*, 1(1), 11-24.
- Jalil, A., Fathani, T. F., Satyarno, I., & Wilopo, W. (2021). Liquefaction in Palu: the cause of massive mudflows. *Geoenvironmental Disasters*, 8(1), 21. <https://doi.org/10.1186/s40677-021-00194-y>.
- Rahman, M. M. (2025). GIS based allowable bearing capacity thematic maps of shallow foundation for Bogura District, Bangladesh. *International Journal of Engineering and Geosciences*, 10(3), 329-338. <https://doi.org/10.26833/ijeg.1589939>
- BNBC. (2020). *Bangladesh National Building Code*.
- Sonmez, H. (2003). Modification of the liquefaction potential index and liquefaction susceptibility mapping for a liquefaction-prone area (Inegol, Turkey). *Environmental Geology*, 44(7), 862-871. <https://doi.org/10.1007/s00254-003-0831-0>.